Fabrication and Properties of VO_x-Based Nanorods

Liqiang Mai,[†,‡] Wanli Guo,[†] Bin Hu,[†] Wei Jin,[†] and Wen Chen*[,†]

State Key Laboratory of Advanced Technology for Materials Synthesis and Processing, School of Materials Science and Engineering, Wuhan University of Technology, Wuhan, 430070, China, and School of Materials Science and Engineering, Georgia Institute of Technology, Atlanta, Georgia 30332-0245

Received: August 27, 2007; In Final Form: October 28, 2007

There is an explosive interest in rodlike vanadium oxide nanomaterials. This review discusses the current research activities on vanadium oxide nanorods in our group. We begin this paper with a variety of chemical and physical methods that have been used to synthesize vanadium oxide nanorods. There follows a discussion of techniques for adjusting vanadium oxide nanorods by doping, ordered constructing, Langmuir−Blodgett assembly, etc. At the end of this paper, we discuss a wide range of interesting properties, such as electrochemical, electrical, optical, magnetic, and field-emission properties, associated with vanadium oxide nanorods, as well as various intriguing applications. We conclude with personal remarks on the outlook for research on vanadium oxide nanorods.

1. Introduction

One-dimensional (1D) nanometer-scale inorganic materials, such as nanowires,[1−6] nanorods,[7−11] and nanotubes,[12−15] have recently attracted much attention because such nanostructures are expected to have unusual characteristics that are amplified through quantum size and shape-specific effects. Vanadium oxide and their derivated compounds are of increasing interest and have been extensively investigated due to their outstanding structural flexibility combined with chemical and physical properties[16,17] and also because of potential applications in areas such as high-energy lithium batteries,[18,19] electrical,[20] magnetic,[21,22] and optical devices.[23,24] Herein, we mainly present the work of our research group on synthesis, controlling, and adjustment of properties of vanadium oxide nanorods. For the sake of clarity, all nonhollow anisotropic vanadium oxide nanostructures will be addressed as "nanorods" in the following, which may have been termed rod, wire, belt, or fiber before, and the nanorods of vanadium oxide-derivated compounds will also be included.

2. Preparation of Vanadium Oxide Nanorods

2.1. Synthesis of Vanadium Oxide Nanorods. *2.1.1. Hydrothermal Process.* As one of the effective routes to the fabrication of high quality vanadium oxide nanorods, the hydrothermal method utilizes a solvent under pressures and temperatures above its critical point to increase the solubility of a solid and to speed up reactions between solids.[25] It provides a commonly used methodology for generating one-dimensional nanostructures. The major advantage of this approach is that most materials can be made soluble in a proper solvent by heating and pressurizing the system close to its critical point, and it should be well-suited for use with any solid material.

Monoclinic $NH_4V_3O_8$ single-crystalline nanorods with widths of 80−180 nm, thicknesses of 50−100 nm, and lengths up to tens of micrometers have been synthesized at large scale in an ammonium metavanadate solution by a template-/catalyst-free route.[16] Such nanorods grow along the direction of [010] (Figure 1). Wang et al. synthesized single-crystalline $LaVO_4$ nanorods[22] and $LaVO_4$/Eu nanorods[26] by an EDTA-mediated hydrothermal method. These nanorods were rodlike in shape with diameters of ∼100 nm, and their lengths were in the range of ∼0.5−1 μm, and they were structurally uniform and free from defects and dislocations.

2.1.2. Rheological Self-Assembling. Rheological self-assembling is a process of combining the self-assembly technique with the rheological phase reaction,[27] which is a new method to synthesis one-dimensional nanomaterials. The main advantages of the rheological self-assembling method are (a) the surface area of solid particle can be efficiently utilized; (b) the contact between solid particle and liquid is close and uniform; (c) heat exchange is very good, and local overheating can be avoided; (d) the reaction temperature is easy to control; and (e) many substances exhibit new reaction properties in this state.[28]

Novel B phase vanadium dioxide nanorods were synthesized for the first time using V_2O_5 powder as precursor and cetyltrimethyl ammonium bromide (CTAB) as template via the rheological self-assembling process.[29,30] The mixture was stirred for 48 h in air. The resulting rheological suspension was transferred into a Teflon-lined autoclave with a stainless steel shell. The autoclave was kept at 180 °C for about a week. The attained products are monoclinic (*C*/2*m*) B phase VO_2 nanorods and they are ∼1−2 μm in length (Figure 2a). HRTEM images reveal that they indeed form bundles of agglomerated smaller filaments with diameters ranging from 20 to 40 nm (Figure 2b) in addition to single nanorods (Figure 2c). This filament-like shape in the nanoscale dimension leads to the exposure of a large fraction of the atoms to the surface. Thus, these materials are promising candidates for the development of new functionalized materials.[31]

Moreover, Chen et al. prepared the M phase VO_2 nanorods through a phase-transfer process of VO_2 (B) → VO_2 (R) → VO_2 (M) by treating B phase VO_2 nanorods with H_2O_2 and CTAB solution.[32]

2.1.3. Microemulsion Method. Microemulsion systems have been widely used as ideal media to prepare nanoparticles. A water-in-oil (w/o) microemulsion is a transparent and isotropic

* Corresponding author. E-mail: chenw@whut.edu.cn.
† Wuhan University of Technology.
‡ Georgia Institute of Technology.

10.1021/jp076849k CCC: $40.75
Published on Web 12/15/2007

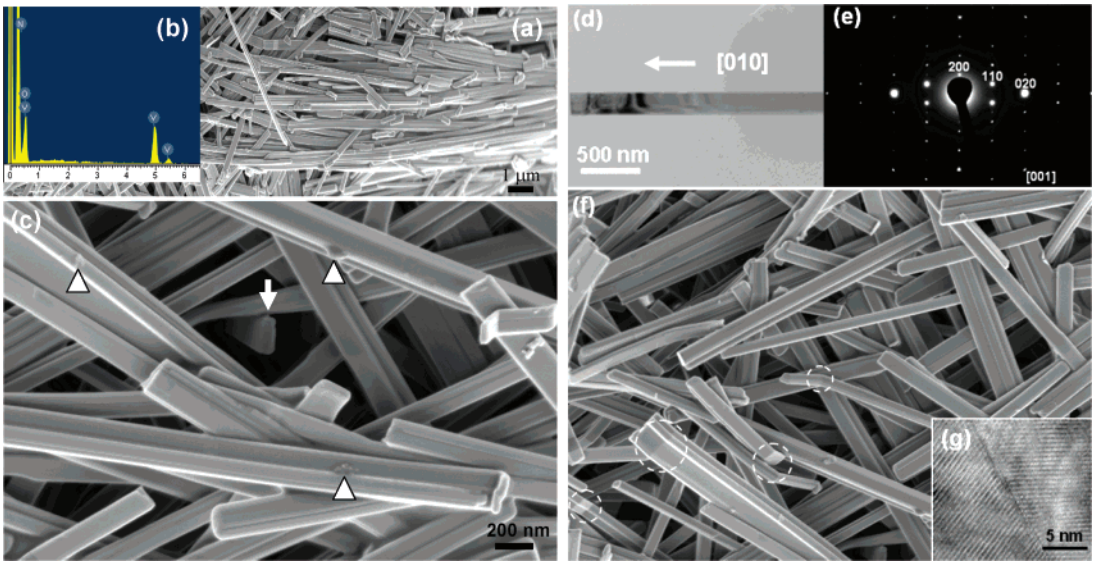

Figure 1. Low magnification SEM image (a), EDS spectrum (b), and high magnification SEM image (c) of $NH_4V_3O_8$ nanorods. In part c, the arrows indicate the rectangular ends of the nanobelts, and the triangles show some bulk and surface defects. TEM image (d) and the corresponding selected area electron diffraction (SAED) pattern (e) of a $NH_4V_3O_8$ nanorod. (f) SEM image of the bent or twinned $NH_4V_3O_8$ nanorods, which are marked by a circle. (g) The representative HRTEM image of the twin boundary present in a nanorod (reprinted by permission from ref 16).

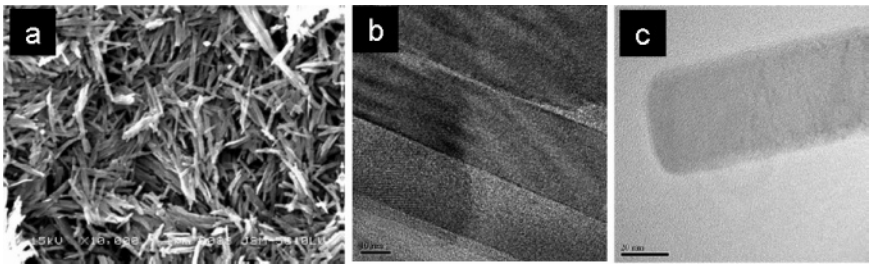

Figure 2. SEM image of VO_2 (B) naorods (a); transmission electron microscopic (TEM) images of VO_2 (B) bundle (b) and individual nanorod (c) (reprinted by permission from ref 29).

liquid medium with nanosized water pools dispersed in a continuous phase and can be stabilized by surfactant and cosurfactant molecules at the water−oil interface. These water pools offer ideal microreactors for the formation of nanoparticles. At present, it can also be used to prepare some 1D nanostructures under certain conditions. A large variety of nanorods have been prepared in microemulsions. These include CeO_2, $SrTiO_3$, $BaTiO_3$, SnO_2, $BaWO_4$, $BaCrO_4$, $NiTiO_3$, Bi_2O_3, $CaSO_4$, Ag, CdSe, and others. Recently, our group prepared vanadium oxide nanorods using a reverse micelle technique, as show in Figure 3. The water content (w), defined as the ratio of water to surfactant concentration, was kept constant at 16. The attained nanorods have a diameter of ∼2−5 nm and a length of ∼100−200 nm.

2.1.4. Template-Directed Method. Various techniques have been established for synthesizing one-dimensional nanostructures, such as nanowires and nanorods.[33,34] Among them, template-directed synthesis is one of the most common fabrication methods, particularly for mass production and alignment. Nanorods of numerous materials, including metals, polymers, oxides, and composites, have been formed using this technique.[35−38] Recently, we synthesized vanadium oxide nanorods by polycarbonate template, and Figure 4 shows the morphology of vanadium oxide nanorods after removing the polycarbonate. In this method, a porous membrane, such as polycarbonate or anodic alumina, is used as a template and precursor of desired material. Filling of template pores could be achieved by capillary forces, electric field, centrifugation force, chemical vapor deposition, and so on.[39] Electric field has been used for both

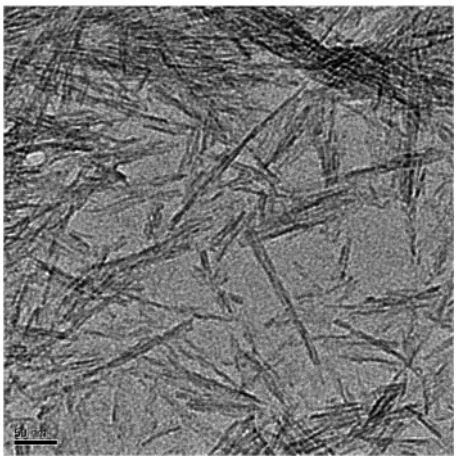

Figure 3. TEM image of vanadium oxide nanorods synthesized in reverse micelles.

electrochemical and electrophoretic deposition. Electrochemical deposition, also commonly referred to as electrodeposition, is generally used for the growth of electrically conductive materials, such as metals, semiconductors, and conductive polymers.[35] The major difference between electrophoretic deposition and electrochemical deposition is that the material deposited by electrophoretic deposition need not be electrically conductive. Electrophoretic deposition simply uses such an oriented motion of charged particles to grow monoliths (e.g., nanorods) by enriching the solid particles from a colloidal dispersion or a sol onto the surface of an electrode.[40]

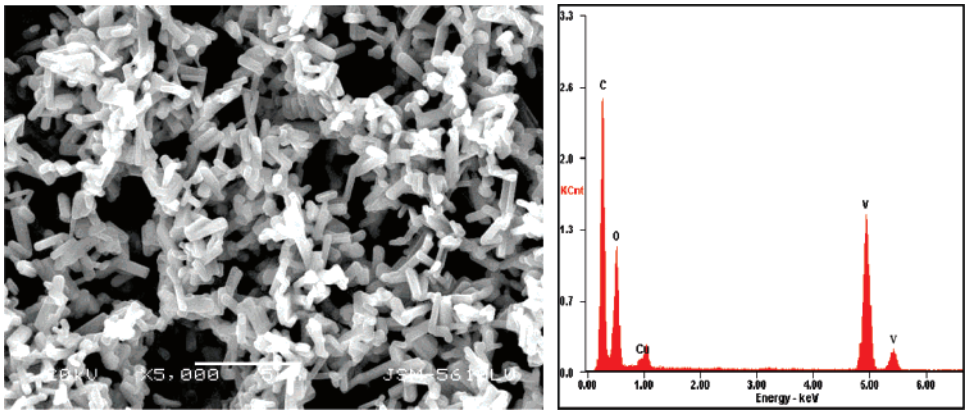

Figure 4. SEM image of vanadium oxide nanorods (left) and the corresponding EDS pattern of the nanorods (right).

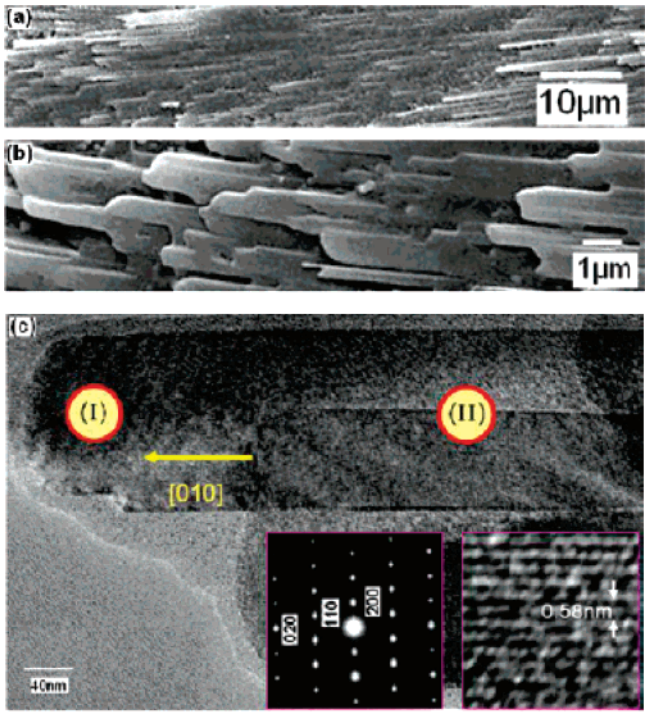

Figure 5. Low (a) and high (b) magnification SEM of Mo-doped VO_2 nanorod array film. (c) TEM image of a Mo-doped VO_2 nanorod. The left and right insets are the corresponding selected area electron diffraction and lattice fringe, respectively (reprinted by permission from ref 20).

2.2. Controlling and Adjustment of Vanadium Oxide Nanorods. *2.2.1. Doping.* Doping is an important method for enforcing and adjusting the properties and performance of materials. Aligned nanorod film of Mo-doped VO_2 has been prepared by simple melting−quenching followed by heat treatment in a vacuum(Figure 5).[20] The new microstructure is formed by the cleavage along the (001) and (100) planes of the oxide lamella inherited from the layered structure of the vanadium oxide xerogel film. The Mo-doped VO_2 nanorod array film shows a low semiconductor-to-metal (S−M) transition temperature of 42 °C and a narrow hysteresis loop of 2 °C. In hydrothermal synthesis of YVO_4 nanorods and microtubes using $(NH_4)_{0.5}V_2O_5$ nanorod templates, when doped with 5 mol % Eu^{3+}, the samples can produce PL properties.[41] Volkov et al. prepared titanium-doped vanadium oxide nanorods of composition $V_{0.95}Ti_{0.05}O_{2.33}(C_6H_4)_{0.12}$ from the $V_{1.67}Ti_{0.33}O_{4.84}{\cdot}nH_2O$ gel/hydroquinone (HQ) composite for 30−50 h at 150−180 °C.[42] They found that when poly(vinyl alcohol) was added to the gel instead of HQ, single nanorods 35 nm in diameter and 500 nm long, oval nanoparticles, and fibrous species were formed. Tetragonal phased $LaVO_4$/Eu was synthesized via an ethylenediamine tetraacetic acid EDTA- assisted hydrothermal method.[43] The challenging transformation from monazite to the metastable zircon structure for $LaVO_4$/Eu resulted in a remarkable improvement of the luminescent properties. This improvement was rationally analyzed, and the impact of structure on the luminescent properties was explored. On the basis of these results, improvement of structural transformation-induced luminescent properties was proposed as an efficient means to improve the performance of doped-insulators.

2.2.2. Ordered Constructing. Ordered constructing is very important for adjusting and improving the properties of 1D nanomaterials and speeding their application.[44] Template directing is still one of the widely used methods in ordered constructing.[45] Nowadays, the templates mainly are porous anodic alumina, polymer, and nanochannel glass templates. And among them, polycarbonate (PC) templates are very convenient to remove by organic solvent or thermal treatment, especially for amphoteric oxide V_2O_5. For instance, Limmer et al. prepared V_2O_5 nanorod arrays using complex direct electrochemical deposition in PC membranes.[24]

On the basis of our previous method,[46] our group has fabricated V_2O_5 nanorod arrays by using cheaper and more accessible V_2O_5 powder as the raw material, combining sol−gel chemistry and PC membrane. The corresponding low-magnification scanning electron microscope (SEM) image of the sample after heat treatment is shown in Figure 6a. From the image and its inset, which is another SEM image of the sample, it can be revealed that the as-grown $V_2O_5{\cdot}nH_2O$ nanostructure has a one-dimensional array morphology on the glass slide substrate. It can also be seen that the length of the nanorod is more than 5 μm, which corresponds to the thickness of the PC membrane. Typical TEM image of the single nanorod is shown in Figure 6c, from which the solid structure of the nanorod can be clearly recognized. From that, it can also be seen that the diameter of the nanorod is about 200 nm, corresponding to the diameter of pores of PC template. The corresponding HRTEM image of the as-synthesized product (Figure 6d) indicates the nanorod is crystalline $V_2O_5{\cdot}nH_2O$ because it exhibits the well-defined lattice fringes with the lattice spacing measured at 3.1 ± 0.05 Å, which corresponds to the distance between the $(\bar{1}12)$ planes in monoclinic $V_2O_5{\cdot}3H_2O$. The corresponding FFT image also confirms the nature of $V_2O_5{\cdot}3H_2O$ crystals in the as-prepared products. Energy dispersive spectroscopy (EDS) pattern of the nanorods (Figure 6b) confirms the vanadium oxide composition of the as-grown products.

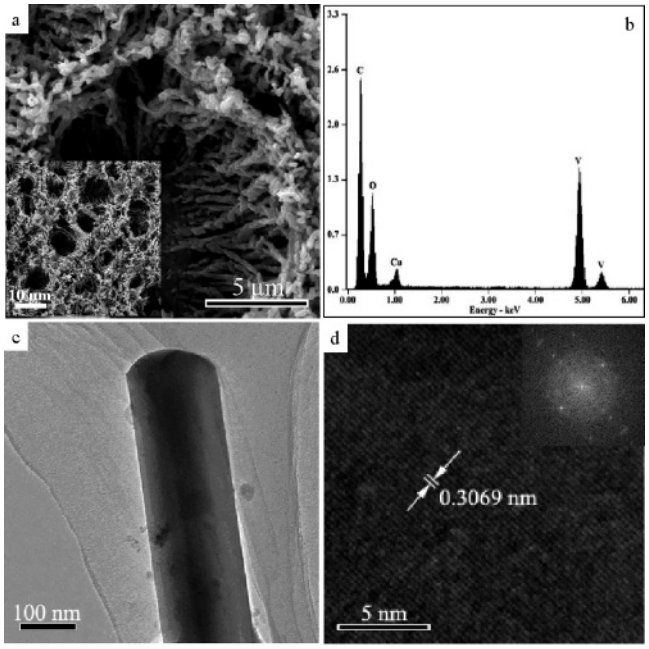

Figure 6. (a) Top view of SEM image of vanadium oxide nanoarrays (the inset is another image of the nanoarrays). (b) EDS pattern of the $V_2O_5 \cdot nH_2O$ nanorods after heat treatment. (c) TEM image of an isolated $V_2O_5 \cdot nH_2O$ nanorod after heat treatment. (d) HRTEM image of the $V_2O_5 \cdot nH_2O$ nanorod after heat treatment (the inset is the corresponding FFT image).

2.2.3. Langmuir-Blodgett Assembly. The Langmuir−Blodgett technique can be used to assemble large areas of nanorod monolayers on a water surface.[47] The monolayer area is limited only by the number of nanorods dispersed on the trough surface. This type of large-scale nanorod assembly is unprecedented and offers a flexible pathway for the step-by-step assembly of virtually any nanorod material into the highly integrated and hierarchically organized nanodevices that are needed for a broad range of functional nanosystems. Yang et al. first applied the Langmuir−Blodgett technique on 1-D nanostrctures.[48] They succeeded in assembling short aspect-ratio nanorods on a water surface to create textures that resembled liquid crystals. Up to now, Langmuir−Blodgett films of various 1-D nanostrctures such as C nanotubes,[49−51] $BaWO_4$ nanorods,[52] ZnSe nanowires and nanorods,[53−55] Ag nanowires,[56] and Ge nanowires[57] have been prepared. Especially, Lieber et al. had used this method to prepare nanowire masks from nanometer- to micrometer-scale pitches for deposition and etching.[58,59]

We have used this technique to assemble VO_2 nanorods as shown in Figure 7. VO_2 nanorods were functionalized and rendered hydrophobic and monodispersed in chloroform via melted stearic acid toluene solution, followed by microemulsion. These nanorods floating on the water self-rotate around their central axis till the (00*l*) crystal planes are paralleled to the water/air interface on the basis of hydrogen bonds between the subphase (deionized water) and (00*l*) crystal plane of VO_2 nanorods, which results in the formation of a (001) crystal plane orientation VO_2 nanorod Langmuir−Blodgett film. Otherwise, using the Langmuir−Blodgett technique, a local area aligned nanorod film was assembled. This well-assembled film may have potential application in many fields, such as nanosystems for electronics and optics and masks for deposition and etching.

3. Properties of Vanadium Oxide Nanorods

3.1. Electrochemical Property. Energy storage is one of the great challenges in the current century due to the emerging energy resource crisis and ecological concerns. It is critical that low-cost, lightweight, small-volume, and environmentally friendly energy storage/conversion devices be developed, and nanomaterials are attracting great interest for electrochemical energy storage due to their large surface area; for example, rechargeable lithium ion batteries. They are considered to be the most advanced energy storage systems. Vanadium oxides belong to the family of semiconducting oxides and have an interesting layered structure that permits a wide variety of other molecules or cations to be embedded between the layers. This makes the 1D vanadium oxide nanorods likely to be good Li ion battery materials.

Chen et al. investigated the electrochemistral properties of pure and Mo-doped VO_2 (B) nanorods made by the rheological self-assembling process[32] and reported that the specific charge and discharge capacity for the VO_2 (B) nanorods are 254 and 247 mAh/g and for VO_2 (B) with Mo doping content of 1 mol % are 276 and 268 mAh/g, respectively. The capacity of undoped and Mo doped VO_2 (B) nanorods remained 224 and 258 mAh/g after 10 cycles. In contrast to normal VO_2 crystal material, whose reversible capacity is ∼160 mAh/g, VO_2 nanorods possess better electrochemical properties (Figure 8). Vanadium oxide nanorods possess better electrochemical properties than conventional bulk materials due to their large surface area, the short diffusion length of Li ions, and their stable microstructure. In an intensive search for alternative materials of commercial cells, which utilize cobalt-based oxides as the positive electrode, but the high cost and toxicity of which prohibit use in large-scale application, vanadium oxide nanorods become one of the most promising.

3.2. Electrical Transport. Among many typical transition metal oxides, vanadium oxides have the special arrangement of extranuclear electrons, and vanadium oxide nanorods have attracted increasing attention as functional units for mediating the transport of electrons.[60] The fundamental study of the electrical properties of vanadium oxide nanorods is crucial for developing their future applications in nanoelectronics.[61]

Mai et al. investigated the electrical transport properties of $NH_4V_3O_8$ nanorods with a rectangular cross section.[16] The individual $NH_4V_3O_8$ nanobelt exhibits nonlinear, symmetric current/voltage (I/V) characteristics, with a conductivity of 0.1−1 S/cm at room temperature and a dielectric constant of ∼130. The dominant conduction mechanism is based on a small polaron hopping due to ohmic mechanism at low electric field below 249 V/cm, which is due to Schottky emission at medium electric field between 249 and 600 V/cm and due to the Poole−Frenkel emission mechanism at high field above 600 V/cm.

The electrical property of Mo-doped VO_2 nanowire array film was also investigated.[20] The results show the S−M transition temperature decreases, and the magnitude of the conductivity change across the transition decreases from 3.9 orders of magnitude for the undoped sample to 3.4 orders of magnitude for the Mo-doped film. This result is explained by the higher conductivity of the semiconducting state of Mo-doped VO_2 films, which results from the enhancement of the carrier concentration due to the presence of Mo donors.

The following relation is used to link the activation energy $E_a = E_c - E_f$ to the temperature coefficient of resistance (TCR) to explain the mechanism,

$$E_a = -kT^2 \times \mathrm{TCR}$$

where E_c is the energy of the edge of the conduction band, E_f is the Fermi level, and k is the Boltzmann constant.

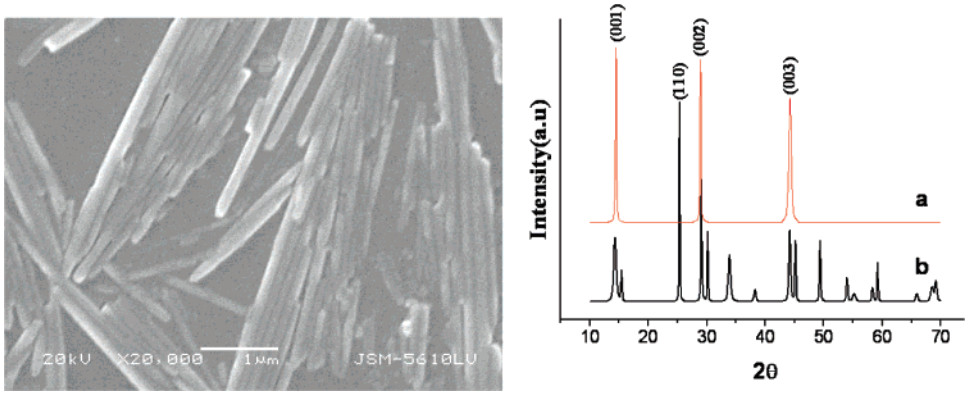

Figure 7. Typical SEM images of Langmuir−Blodgett films (left). The X-ray diffraction patterns of VO_2 nanorod Langmuir−Blodgett films (a) and as-synthesized VO_2 nanorods (b) (right).

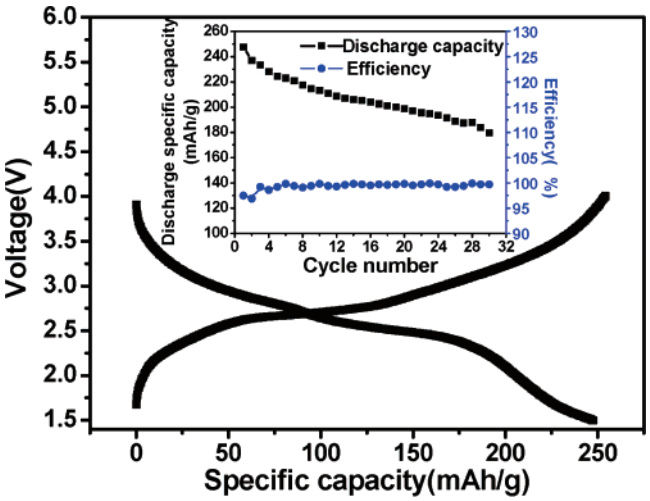

Figure 8. Initial charge/discharge curve of VO_2 (B) nanorods (the inset is the curves of their specific capacity and efficiency vs cycle number) (reprinted by permission from ref 32).

Measurement values show that undoped VO_2 films have a TCR of about 1.71 ± 0.02%/°C and an E_a of about 0.143 ± 0.004 eV. However, a lower TCR of 1.38 ± 0.02%/°C and activation energy of 0.107 ± 0.004 eV are obtained for the Mo-doped VO_2 films. Mo doping increases the electron density and leads the Fermi energy level shift toward the conduction band. As a result, E_a, hence TCR, decreases.

3.3. Magnetism. Vanadium oxides are frequently of mixed valency, typically V^{4+} and V^{5+}, and often are crystallized into weakly coupled, layered two-dimensional networks. Owing to the interplay of internal degrees of freedom—spin, charge, and orbital—they can suddenly transform from a metal to an insulator (Mott−Hubbard) and become superconducting or host unusual quantum spin states.[62]

Wang et al. studied the magnetic properties of $LaVO_4$/Eu nanorods and $LaVO_4$ nanorods.[26] Upon field cooling, both $LaVO_4$/Eu nanorods and $LaVO_4$ nanorods exhibit antiferromagnetic behavior in certain temperature ranges, just as the prediction according to the Anderson mediate exchange model (Figure 10). But because of the reduced unit cell parameters, T_N of $LaVO_4$/Eu nanorods is about 50 K, which is lower than that of $LaVO_4$ nanorods ($T_N \approx 55$ K). Above T_N, χ_M decreases with increasing temperature. It means that $LaVO_4$/Eu nanorods and $LaVO_4$ nanorods behave as a paramagnetic state due to the existence of three-valence lanthanum. When the temperature is below T_t, χ_M increases with a decrease in the temperature. And they both behave ferromagnetically. The ferrimagnetism can be explained by the trace V^{3+}. With the decrease in the temperature, the V^{3+} ordering leads to the magnetic ordering of V^{3+}.[63] Furthermore, the europium ions doped in the $LaVO_4$ nanorods lead to noticeable improvements in the luminescence properties and the magnetic properties.

3.4. Field Emission Property. Vanadium oxides have versatile redox-dependent properties as a result of the multiple valence state of vanadium, possessing a band gap of not more than 2.9 eV. Vanadium oxide nanorods could exhibit excellent properties because of the large surface area and specific shape, and the corresponding nanoarray structure has a high aspect ratio, large surface areas, and many nanotips, which are very good for FE behaviors.[46] These advantages make them have great application prospects in many fields, one of which may be field emission displays (FED). However, to our knowledge, no report can be found on a FE emitter using V_2O_5 nanorod arrays up to now.

Here, the FE property of aligned $V_2O_5 \cdot nH_2O$ nanorods with sharp nanotips was investigated. The plot of the emission current densities versus electric field for the as-synthesized sample after heat treatment with an emitting surface area of 7.85 mm^2 is shown in Figure 11. The electron emission turn-on field (E_{to}), defined as the macroscopic fields required to produce a current density of 10 $\mu A/cm^2$ is ~7.31 V/μm. In general, according to the standard of Samsung Corporation, the emission current density for industrial video graphics array field emission displays (VGAFED) is 1 mA/cm^2, and the maximum emission current density of the present nanorod arrays is 1.9 mA/cm^2 at a field of 11.81 V/μm, so it can be indicated that the as-synthesized nanorod arrays possess good FE properties.

It is known that at room temperature, the emission current mostly originates from the tunneling of electrons through the surface barrier, which is described by the Fowler−Nordheim (F−N) theory. The emission current can be expressed in terms of the experimental parameters in the following equation,

$$\ln\left(\frac{I}{V^2}\right) = \frac{1}{V}(-6.8 \times 10^7 \alpha R_{tip} \Phi^{3/2}) + \text{offset}$$

where I is the current density, V is the applied field, R_{tip} is the tip radius of curvature, α is a modifying factor, and Φ is the work function. The F−N plot of ($\ln I/V^2$) versus ($1/V$) is represented in the inset of Figure 11. It is interesting to reveal that the F−N plot has a linear relationship of a two-stage slope, which implies that the field emission from the $V_2O_5 \cdot nH_2O$ nanorod arrays follows the FN theory and the emitted current is, indeed, caused by quantum tunneling.[64,65] The results indicate that the $V_2O_5 \cdot nH_2O$ nanorod array can be a promising candidate

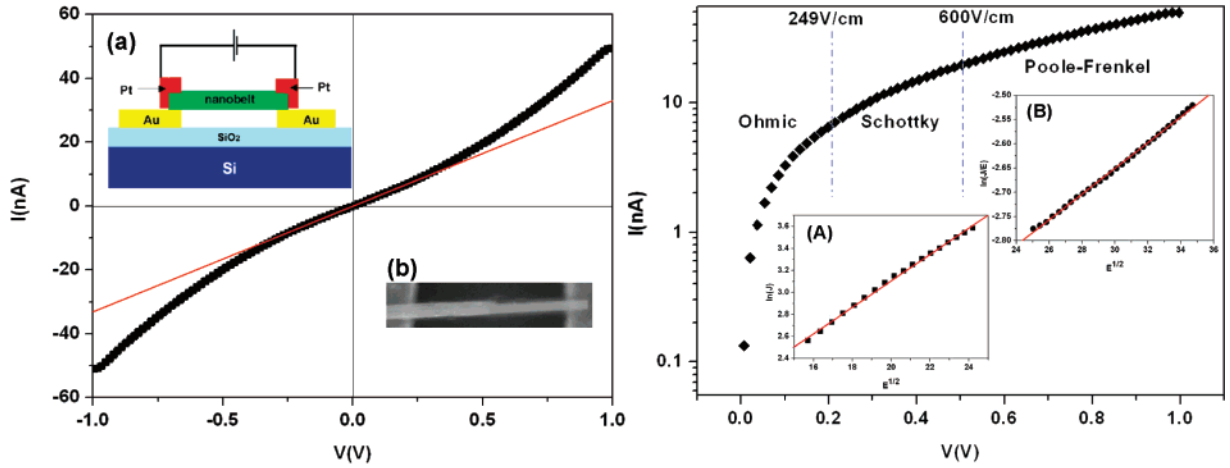

Figure 9. I−V curve of individual nanobelt. The insets a and b show a schematic view and the SEM image of the individual nanobelt electrode, respectively (left). The positive part of the I−V characteristics of the transversal system, rebuild as a function of log(*I*). Insets A and B show the experimental plot of ln(*J*) versus $E^{1/2}$ at the electric field between 249 and 600 V/cm, and the experimental plot of ln(*J*/*E*) versus $E^{1/2}$ at a electric field more than 600 V/cm (right) (reprinted by permission from ref 16).

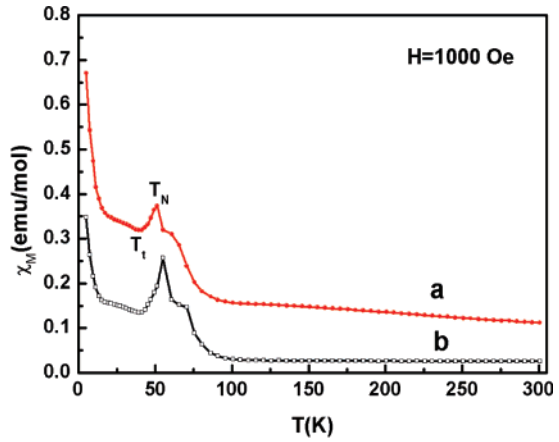

Figure 10. The relationship between the temperature and the susceptibility of the $LaVO_4$/Eu nanorods and pure $LaVO_4$ nanorods: (a) $LaVO_4$/Eu nanorods; (b) $LaVO_4$ nanorods (reprinted by permission from ref 22).

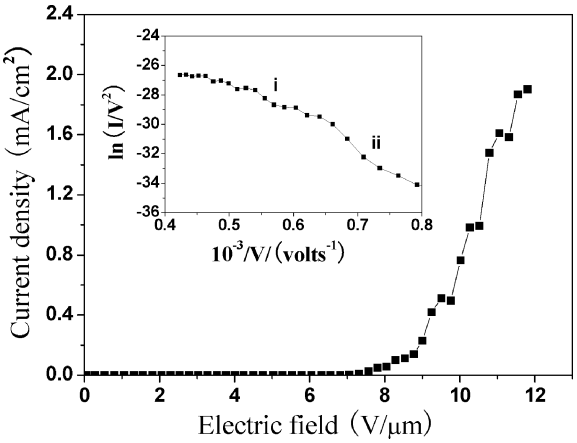

Figure 11. Typical FE current density vs electric field curve for the $V_2O_5 \cdot nH_2O$ nanorod arrays (the insert is the corresponding F−N plot).

as a FE emitter because of the unique structure and electrical properties of the present V_2O_5 nanorods.

4. Concluding Remarks

Recent advances of our research group on vanadium oxide nanorods have been summarized here. Different methods, such as the hydrothermal method, rheological self-assembling, the microemulsion technique, and the template-directed method, were used to prepare vanadium oxide nanorods. The wide range of interesting properties, such as electrochemical, electrical, optical, magnetic, field-emission properties, associated with vanadium oxide nanorods was also investigated. There are also some challenges remaining. The first challenge is the growth and fabrication of nanoscale p−n junctions based on vanadium oxide nanorods for electrically driven nano-optoelectronics. The second challenge is integration of vanadium oxide nanorod building blocks for large-scale device applications. The third challenge is to demonstrate radically new applications for vanadium oxide nanorods. Processing methods in this review are generally applicable to fabricating and asembling nanostructures of other oxides; for example, metal oxide coreshell nanocable arrays. A discussion on the underlying principle that affects the properties of vanadium oxides in the present work can be helpful for further understanding of vanadium oxides and other transition metal oxides. Considering that vanadium oxides possess versatile redox-dependent properties, one can foresee the tremendous possibility and potential of constructing multifunctional and hybrid nanodevices based on vanadium oxide nanorods.

Acknowledgment. This work was supported by the National Nature Science Foundation of China (50702039, 50772085, 50672071, 50672072); the Key Project of the Chinese Ministry of Education (105124); Program for Changjiang Scholars and Innovative Research Team in University (PCSIRT, No. IRT0547), Ministry of Education, China; the Foundation for Innovation Research Team (2005ABC004) and the Natural Science Foundation (2006ABA310) of Hubei Province; and the Wuhan Youth Chenguang Project (20065004116-17). The authors thank Nian Wang, Chiwei Zhou, Yimin Wu, Bo Hu, and Yuan Gao for their assistance. The authors are pleased to thank Professor Z. L. Wang for giving good suggestions and helping to revise the manuscript.

References and Notes

(1) Wu, Y.; Xiang, J.; Yang, C.; Lu, W.; Lieber, C. M. *Nature* **2004**, *430*, 704−704.
(2) Hannon, J. B.; Kodambaka, S.; Ross, F. M.; Tromp, R. M. *Nature* **2006**, *440*, 69−71.
(3) Mai, L. Q.; Hu, B.; Chen, W.; Qi, Y. Y.; Lao, C. S.; Yang, R. S.; Dai, Y.; Wang, Z. L. *Adv. Mater.* **2007**, *19*, 3712−3716.
(4) Tosatti, E.; Prestipino, S. *Science* **2000**, *289*, 561−563.

(5) Schmidt, V.; Gosele, U. *Science* **2007**, *316*, 698−699.
(6) Ng, H. T.; Li, J.; Smith, M. K.; Nguyen, P.; Cassell, A.; Han, J.; Meyyappan, M. *Science* **2003**, *300*, 1249−1249.
(7) Naumov, I. I.; Bellaiche, L.; Fu, H. X. *Nature* **2004**, *432*, 737−740.
(8) Xiong, Y. J.; Cai, H. G.; Wiley, B. J.; Wang, J. G.; Kim, M. J.; Xia, Y. N. *J. Am. Chem. Soc.* **2007**, *129*, 3665−3675.
(9) Liu, B.; Zeng, H. C. *J. Am. Chem. Soc.* **2003**, *125*, 4430−4431.
(10) Imura, K.; Nagahara, T.; Okamoto, H. *J. Am. Chem. Soc.* **2004**, *126*, 12730−12731.
(11) Cheng, B.; Russell, J. M.; Shi, W. S.; Zhang, L.; Samulski, E. T. *J. Am. Chem. Soc.* **2004**, *126*, 5972−5973.
(12) Remskar, M.; Mrzel, A.; Skraba, Z.; Jesih, A.; Ceh, M.; Demsar, J.; Stadelmann, P.; Levy, F.; Mihailovic, D. *Science* **2001**, *292*, 479−481.
(13) Cohen, A. E. *Science* **2003**, *300*, 1235−1235.
(14) Mai, L. Q.; Chen, W.; Xu, Q.; Zhu, Q. Y.; Han, C. H.; Peng, J. F. *Solid State Commun.* **2003**, *126*, 541−543.
(15) Mai, L. Q.; Chen, W.; Xu, Q.; Peng, J. F.; Zhu, Q. Y. *Chem. Phys. Lett.* **2003**, *382*, 307−312.
(16) Mai, L. Q.; Lao, C. S.; Hu, B.; Zhou, J.; Qi, Y. Y.; Chen, W.; Gu, E. D.; Wang, Z. L. *J. Phys. Chem. B* **2006**, *110*, 18138−18141.
(17) Mai, L. Q.; Chen, W.; Qi, Y. Y.; Dai, Y. *Solid State Phenom.* **2007**, *121*−*123*, 789−792.
(18) Nordlinder, S.; Edstrom, K.; Gustafsson, T. *Electrochem. Solid State* **2001**, *4*, A129−a131.
(19) Liu, P.; Zhang, J. G.; Tracy, C. E.; Turner, J. A. *Electrochem. Solid State* **2000**, *3*, 163−166.
(20) Mai, L. Q.; Hu, B.; Hu, T.; Chen, W.; Gu, E. D. *J. Phys. Chem. B* **2006**, *110*, 19083−19086.
(21) Luo, F.; Song, W.; Li, Z. F.; Yan, C. H. *Solid State Commun.* **2004**, *132*, 595−599.
(22) Wang, N.; Zhang, Q. F.; Chen, W. *Cryst. Res. Technol.* **2007**, *42*, 138−142.
(23) Lopez, R.; Feldman, L. C.; Haglund, R. F. *Phys. Rev. Lett.* **2004**, *93*, 1774031−1774034.
(24) Takahashi, K.; Limmer, S. J.; Wang, Y.; Cao, G. Z. *J. Phys. Chem. B* **2004**, *108*, 9795−9800.
(25) Xia, Y. N.; Yang, P. D.; Sun, Y. G.; Wu, Y. Y.; Mayers, B.; Gates, B.; Yin, Y. D.; Kim, F.; Yan, Y. Q. *Adv. Mater.* **2003**, *15*, 353−389.
(26) Wang, N.; Chen, W.; Zhang, Q. F.; Dai, Y. *Mater. Lett.* **2007**, in press.
(27) Mariette, F.; Lucas, T. *J. Agric. Food Chem.* **2005**, *53*, 1317−1327.
(28) Koenig, A.; Hebraud, P.; Perrin, P. *Langmuir* **2002**, *18*, 6458−6461.
(29) Mai, L. Q. Dissertation for Ph.D., Wuhan University of Technology, 2004.
(30) Chen, W.; Mai, L. Q.; Qi, Y. Y.; Jin, W.; Hu, T.; Guo, W. L.; Dai, Y.; Gu, E. D. *Key Eng. Mater.* **2007**, *336*−*338*, 2128−2133.
(31) Mai, L. Q.; Chen, W.; Xu, Q.; Peng, J. F.; Zhu, Q. Y. *Intl. J. Nanosci.* **2004**, *3*, 225−231.
(32) Chen, W.; Mai, L. Q.; Qi, Y. Y.; Dai, Y. *J. Phys. Chem. Solids* **2006**, *67*, 896−902.
(33) McIlroy, D. N.; Zhang, D.; Kranov, Y.; Norton, M. G. *Appl. Phys. Lett.* **2001**, *79*, 1540−1542.
(34) Pan, Z. W.; Dai, Z. R.; Wang, Z. L. *Science* **2001**, *291*, 1947−1949.
(35) Martin, C. R. *Science* **1994**, *266*, 1961−1966.
(36) Whitney, T. M.; Jiang, J. S.; Searson, P. C.; Chien, C. L. *Science* **1993**, *261*, 1316−1320.
(37) Huczko, A. *Appl. Phys. A* **2000**, *70*, 365−376.
(38) Penner, R. M.; Martin, C. R. *J. Electrochem. Soc.* **1986**, *133*, 2206−2207.
(39) Kyotani, T.; Tsai, L. *Chem. Mater.* **1996**, *8*, 2109−2113.
(40) Wang, Y.; Cao, G. Z. *Chem. Mater.* **2006**, *18*, 2787−2804.
(41) Wu, X. C.; Tao, Y. R.; Mao, C. J.; Liu, D. J.; Mao, Y. Q. *J. Cryst. Growth* **2006**, *290*, 207−212.
(42) Volkov, V. L.; Zakharova, G. S.; Volkova, E. G.; Kuznetsov, M. V. *Russ. J. Inorg. Chem.* **2006**, *51*, 847−851.
(43) Jia, C. J.; Sun, L. D.; Luo, F.; Jiang, X. C.; Wei, L. H.; Yan, C. H. *Appl. Phys. Lett.* **2004**, *84*, 5305−5307.
(44) Chen, Z.; Gao, Q. M.; Ruan, M. L.; Shi, J. L. *Appl. Phys. Lett.* **2005**, *87*, 093113−093115.
(45) Yu, H.; Chen, W.; Dai, Y.; Mai, L. Q.; Qi, Y. Y.; Peng, J. F. *J. Wuhan Univ. Technol., Mater. Sci. Ed.* **2006**, *21*, 38−41.
(46) Zhou, C.; Mai, L.; Liu, Y.; Qi, Y.; Dai, Y.; Chen, W. *J. Phys. Chem. C* **2007**, *111*, 8202−8205.
(47) Yang, P. D. *Nature* **2003**, *425*, 243−244.
(48) Kim, F.; Kwan, S.; Akana, J.; Yang, P. D. *J. Am. Chem. Soc.* **2001**, *123*, 4360−4361.
(49) Sano, M.; Kamino, A.; Okamura, J.; Shinkai, S. *Langmuir* **2001**, *17*, 5125−5128.
(50) Hernandez-Lopez, J. L.; Alvizo-Paez, E. R.; Moya, S. E.; Ruiz-Garcia, J. *J. Phys. Chem. B* **2006**, *110*, 23179−23191.
(51) Li, X. L.; Zhang, L.; Wang, X. R.; Shimoyama, I.; Sun, X. M.; Seo, W. S.; Dai, H. J. *J. Am. Chem. Soc.* **2007**, *129*, 4890−4890.
(52) Kwan, S.; Kim, F.; Akana, J.; Yang, P. D. *Chem. Commun.* **2001**, 447−448.
(53) Acharya, S.; Efrima, S. *J. Am. Chem. Soc.* **2005**, *127*, 3486−3490.
(54) Acharya, S.; Panda, A. B.; Belman, N.; Efrima, S.; Golan, Y. *Adv. Mater.* **2006**, *18*, 210−213.
(55) Panda, A. B.; Acharya, S.; Efrima, S.; Golan, Y. *Langmuir* **2007**, *23*, 765−770.
(56) Tao, A.; Kim, F.; Hess, C.; Goldberger, J.; He, R. R.; Sun, Y. G.; Xia, Y. N.; Yang, P. D. *Nano Lett.* **2003**, *3*, 1229−1233.
(57) Wang, D. W.; Chang, Y. L.; Liu, Z.; Dai, H. J. *J. Am. Chem. Soc.* **2005**, *127*, 11871−11875.
(58) Whang, D.; Jin, S.; Lieber, C. M. *Nano Lett.* **2003**, *3*, 951−954.
(59) Whang, D.; Jin, S.; Wu, Y.; Lieber, C. M. *Nano Lett.* **2003**, *3*, 1255−1259.
(60) Mai, L. Q.; Chen, W.; Xu, Q.; Peng, J. F.; Zhu, Q. Y.; Yu, H. *Rare Metal Mater. Eng.* **2003**, *32*, 748−751.
(61) Chen, W.; Mai, L. Q.; Qi, Y. Y.; Yu, H.; Peng, J. F. *Solid State Chem. Inorg. Mater. V* **2005**, *848*, 389−393.
(62) Krusin-Elbaum, L.; Newns, D. M.; Zeng, H.; Derycke, V.; Sun, J. Z.; Sandstrom, R. *Nature* **2004**, *431*, 672−676.
(63) Munoz, A.; Alonso, J. A.; Casais, M. T.; Martinez-Lope, M. J.; Martinez, J. L.; Fernandez-Diaz, M. T. *J. Magn. Magn. Mater.* **2004**, *272*−*76*, 2163−2164.
(64) Tang, Q.; Li, T.; Chen, X. H.; Yu, D. P.; Qian, Y. T. *Solid State Commun.* **2005**, *134*, 229−231.
(65) Hsieh, C. T.; Chen, J. M.; Lin, H. H.; Shih, H. C. *Appl. Phys. Lett.* **2003**, *83*, 3383−3385.